CFD Modelling of Industrial Powders

Olumuyiwa Owoyemi[1], Paola Lettieri [1] and Roger Place [2]

[1] Department of Chemical Engineering, University College London, Torrington Place, WC1E 7JE London, UK. p.lettieri@ucl.ac.uk-.
[2] Place Associates, 41 West End, Sedgefield, Stockton on Tees, TS21 2BW, UK.

ABSTRACT

In the present study, the Eulerian-Eulerian two fluid continuum model built in CFX 4.4 has been used to model and simulate the fluid dynamics of the mono-dispersed system of two industrial powders. Granular Kinetic theory, which is already available from CFX 4.4, has been used for 2D time-dependent simulations for the mono-dispersed system of the individual materials. Model predictions have been compared with experimental data obtained on pressure, voidage and bed height fluctuations. Furthermore, a new Particle Bed model, which makes use of volume-averaged mass and momentum balances for the fluid and particle phases, is proposed, initially for a mono component system, with the aim of extending the model to the simulation of bimodal mixtures at different weight fractions. A fluid- bed stability analysis has also been performed on a range of mono dispersed Geldart Group A powders using the newly proposed model and subsequently compared with experimental results.

Keywords: Fluidization, CFD, Industrial Powders, bubbling

1 INTRODUCTION

The widespread use of fluidized bed technology can be attributed to the very good mixing that occurs within the bed, which in turn enhances solids and fluid contacting and improves heat and mass transfer (Kunii and Levenspiel, 1989). Fluidization has indeed found use spanning across many industries ranging from the pharmaceutical, refining, and petroleum to the power generation industries. One such industry where extensive use of the technology has been applied is the titanium refining industry where a fluidized bed reactor is used for extracting titanium from naturally occurring ore.

Computational Fluid Dynamics (CFD) is routinely used in a wide variety of industries, including aerospace, automotive, chemical and manufacturing industries. The use of CFD in process industries for example has led to reductions in the cost of product and process developments and optimization activities (by reducing down time). CFD has also found increased use amongst research scientists and engineers who are increasingly employing Computational Fluid Dynamics modelling as a tool to study multiphase systems including fluidization. CFD models that describe gas solid flow systems can be formulated at different levels of mathematical detail. Simulating the individual solid particles, whilst the gas phase is simulated on a length scale larger than that of the particle phase, is referred to as the Lagrangian-Eulerian approach; here the Newtonian equation of motion for each particle is solved separately taking into account direct collisions between particles when it is appropriate. This work is however based on the Eulerian-Eulerian approach where both phases are simulated as continuous and fully interpenetrating, a concept based on the two fluid model (TFM). Many researchers have successfully carried out mono component bubbling bed fluidization simulations of Group B particles using the Eulerian-Eulerian

approach. Some of which include Ding and Gidaspow (1990), Van Wachem et al.(1998) and Lettieri et al.(2003a) .The above mentioned authors have used the two fluid model approach that utilizes the kinetic theory of granular flow (Gidaspow, 1994) description for the solid phase as derived from kinetic theory of gases. This approach is also adopted in this work.

This study is concerned initially with the validation of the computational simulation of two Geldart Group B industrial materials, Natural and Synthetic Rutile particles of diameter 186μm and 156μm and particle density of 4200kg/m^3 and 3200kg/m^3 respectively. These powders are used in titanium refining industry. The initial step of the refining process is carried out in a fluidized bed reactor, in which mixtures of natural and synthetic titanium bearing ores are chlorinated in the presence of coke according to the general reaction.

$$TiO_2 + C + 2Cl_2 \rightarrow TiCl_4 + CO + CO_2$$

The study concludes by proposing a new hydrodynamic model capable of predicting the behaviour of mono dispersed fluidized powders as well as offering the scope for extension to cater for binary mixtures. A fluid-bed stability analysis performed on a range of mono dispersed Geldart Group A powders using the newly proposemodel and compared with experimental results is also presented.

2 EXPERIMENTAL METHODOLOGY

Analytical samples of the material investigated were obtained by riffling of large batches. The mean particle diameter and particle size distribution were determined by sieve analysis. The sieve test was repeated three times and average values were taken. Using a scanning electron microscope (SEM) the surface morphology of the materials under investigation were observed and photographs taken. SEM photographs and particle size distributions of the synthetic rutile are reported in Fig.1 and Fig.2 respectively whilst that of the natural rutile is reported in Fig.3 and Fig. 4. From the S.E.M photographs of both powders (Fig 1 and 3) it can be observed that the natural rutile particles are more irregularly shaped whereas the synthetic rutile is more spherical. The physical properties of both powders are summarized in Table 1

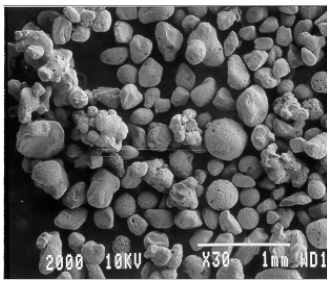

Figure 1 Synthetic Rutile SEM at magnification X=30

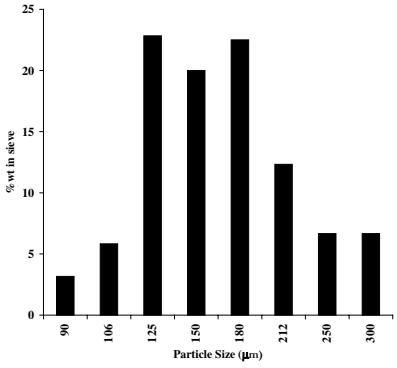

size distribution, d_p = 156μm

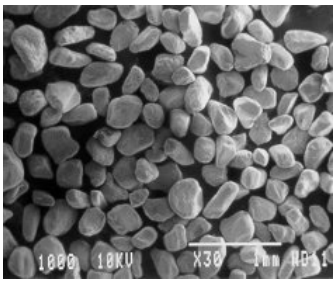

Figure 3 Natural Rutile SEM at magnification X=30

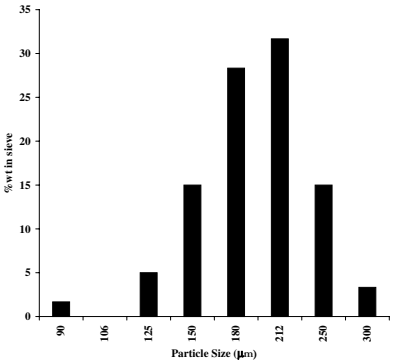

Figure 4 Natural Rutile, particle size distribution, d_p = 186μm

Material	d_p (μm)	ρ_p (kg/m^3)	σ/d_{50}	Geldart Group
Natural Rutile	186	4200	20	B
Synthetic Rutile	156	3200	37	B

Table 1 Particle Physical Properties

The experimental set-up consisted of a two-dimensional plexiglass rectangular column, 600 mm high, 350 mm wide and 10 mm thick. The distributor was a uniformly permeable sintered bronze rectangular plate with a thickness of 3.5 mm. The bed was filled to an initial height of 300 mm, for all experiments, corresponding to 1.89 kg and 1.92 kg of natural and synthetic rutile particles respectively. Fluidizing gas, air, was supplied via rotameters. A mercury manometer was used to measure the pressure drop as a function of the superficial gas velocity to determine the experimental minimum fluidization velocity, U_{mf} for both powders. The minimum fluidization velocity was also calculated using correlations available in literature and subsequently compared with experiments. An agreement of 10% and 30% was found for the synthetic and natural rutile material respectively when experimental measurements and empirical calculations were compared. A record of the bed height at increasing superficial gas velocity enabled the calculation of the bed voidage, which is used also for direct comparison to the CFD simulations. Digital video recordings of the fluid bed were made to analyse the development of bubble dynamics in the fluid bed and determine the bubble size at different fluidizing velocities. Images were captured by means of a web cam at 14 frames/s, 80 s were recorded and were then subsequently analysed using Optimas 6.0, image analysis software. Experiments and corresponding simulations were performed at three different fluidizing velocities that are summarized in Table 2.

Material	Experimental and Simulation Strategy		
	Case A (m/s) Same U_o	Case B (m/s) Same U_o-U_{mf}	Case C (m/s) Same U_{mf}
Natural Rutile	$3U_{mf}$ =0.20	$3U_{mf}$ =0.20	$3U_{mf}$ =0.20
Synthetic Rutile	$8.7U_{mf}$ =0.20	$7U_{mf}$ =0.16	$3U_{mf}$ =0.07

Table 2 Experimental and Simulation Strategies used in this work

3 CFD MODEL

The momentum balance for gas and solid phase is given by the averaged Navier-stokes equations, proposed by Jackson (2001). The Kinetic theory of granular flow (Gidaspow, 1994), available within CFX4.4, was used for closure of the solid phase stress term. The transfer of momentum between the two phases is accounted for via the interphase transfer co-efficient, which can be computed from knowledge of the Drag coefficient, C_D, Reynolds number and the solids volume fraction, ε_s. We report in Table 3 interphase transfer function used in this work.

Interphase transfer function: (Di Felice,1994)

$$\beta = \frac{3}{4} C_D \frac{\rho_f \varepsilon_s \left| \overline{u_f} - \overline{u_s} \right|}{d_p} . (1 - \varepsilon_s)^{2-\gamma}$$

with

$$\gamma = 3.7 - 0.65 e^{\left(-\frac{[1.5 - \log(\varepsilon_g \, \mathbf{Re})]^2}{2} \right)}$$

Drag Coefficient (DallaValle ,1948)

$$C_D = \left(0.63 + 4.8 \, \mathbf{Re}_p^{-0.5} \right)^2$$

Table 3 The Constitutive equations used in the CFD model

4 SIMULATIONS

A rectangular geometry of dimensions equal to the experimental rig was used to set up the computational domain, with gas entering at a uniform velocity at the distributor plate. In this work, all simulations were carried out in a 2-D computational grid in which front and back wall effects are neglected. The left and right walls of the domain were modelled using no-slip velocity boundary condition for both phases. Dirichlet boundary conditions are employed at the bottom of the bed to specify a uniform gas inlet velocity. The boundary condition at the top of the bed is a so-called pressure boundary, which is set to a reference value of 1.015×10^5 Pa. The distributor is made impenetrable for the solid phase. The conditions used in this simulation are summarized in Table 4. All simulations were performed for 5 secs of real time. The simulations using a Dell Xeon P4 3.1 Ghz Machine.

Description	Symbol	Value	Comments
Gas Density	ρ_g [kg/m^3]	1.2	
Gas Viscosity	μ_g [Pa s]	1.85×10^{-5}	
Restitution Coefficient	e	0.90	
Maximum Solids Packing	ε_s, max	0.60	
Bed height	H_{bed} [m]	0.60	
Settled bed height	H_s [m]	0.30	
Grid cell size	Δx and Δy [m]	0.005	Square Cells
Time step	Δt [s]	10^{-4}	Time steps

Table 4 Computational Parameters used in the CFD simulations

5 RESULTS

5.1 Voidage Profile

One of the objectives of this work is to validate results obtained from CFD simulations with experimental results. In this section, snapshots showing the fluidization of the natural and synthetic rutile are compared with voidage contour maps obtained from CFD simulations. Fig.5 and Fig.6 show the voidage profiles for both powders when fluidized at the same gas velocity, U_o = 0.2 m/s (Case A). The bubbles that form in the natural rutile are smaller in comparison to the synthetic rutile, as can be observed in the snapshots reported in Fig.5. This material is characterised by a higher U_{mf} than the synthetic rutile and thus a smaller excess gas velocity at the same superficial gas velocity. The experimental and simulated snapshot of the synthetic rutile, Fig 6, shows a more vigorous bubbling regime when compared to the natural rutile ones. This behaviour is expected because of the lower minimum fluidization velocity of the synthetic rutile material. From the snapshots, it can also be seen that bubbles start to coalesce near the bottom of the bed and increase in size as the process of coalescence develops higher up in the bed.

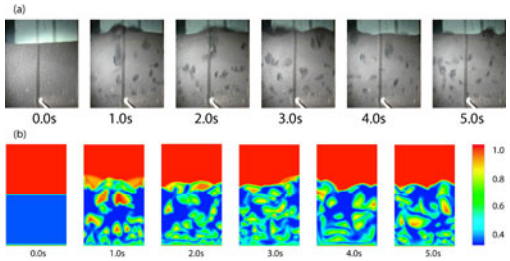

Figure 5 Voidage profile comparison between experimental (a) and simulated (b) Natural Rutile material at U_o=0.2m/s

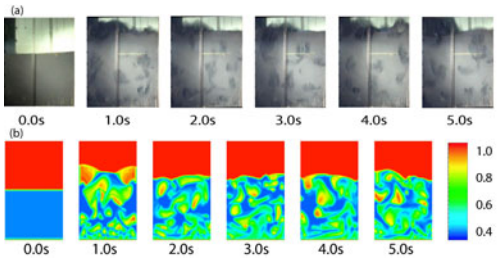

Figure 6 Voidage profile comparison between experimental (a) and simulated (b) Synthetic Rutile material at U_o=0.2m/s (CASE A)

5.2 Bed Expansion

Figure 7, obtained by averaging the values for the bed height at different superficial velocities, shows a good match between experimental and simulated averaged bed expansion, with the simulated values being between 2.5-11% lower than the experimentally measured bed height at the velocities investigated. A possible explanation might be that the actual powder has a wide particle size distribution whilst the simulation was performed assuming a system of monosized particles.

5.3 Bubble properties

In this work, the semi-empirical model for bubble growth proposed by Darton et al.(1977) is used. This equation gives the bubble diameter as a function of the bed height as follows:

$$d_B = 0.54\left(u - u_{mf}\right)^{0.4}\left(h + 4\sqrt{A_o}\right)^{0.8} \Big/ g^{0.2} \qquad (1)$$

where d_b is the bubble diameter, h is the height above the distributor and A_o is the 'catchment area', which characterises the gas distributor. The constant 0.54 has been obtained experimentally. In absence of available data on the distributor characteristics, Darton et al.(1977) suggested a value for A_o equal to 0. This fairly corresponds to the inlet

boundary conditions set-up during this work, where no distributor has been simulated. In defining a bubble, an appropriate voidage has to be selected as the boundary between the emulsion and the gas phase. In this work a voidage contour of 0.80 has been assumed for both experimental and simulation measurements. The analysis of experimental bubble diameter was carried out using Optimas 6.0, image analysis software. A total of 60 bubble diameters were collated from the experimental analysis. Figure 8 shows a comparison between the CFD simulations, experimentally obtained bubble diameter measurements and predictions from Darton's correlation for the synthetic rutile powder. The simulated values are shown to be below the experimental ones, with the scatter between experimental and simulated bubble size being greater at higher heights in the bed. On the other hand, the Darton's correlation always over predicts the bubble size for both materials - In previous work, Cammarata et al.(2003b) had shown similar results when comparing bubble size obtained from 2D and 3D simulations of a Group B material with predictions using the Darton Equation. In this case, results from 2D simulations were always lower than that predicted by Darton.

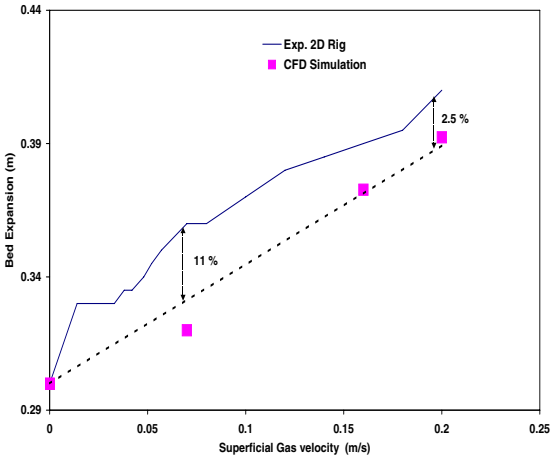

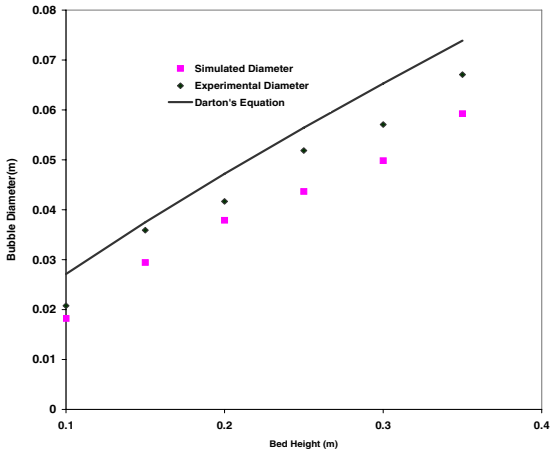

correlation for synthetic rutile material at U_o = 0.2m/s

6 PROPOSED PARTICLE BED MODEL

In this section a new computational fluid dynamics (CFD) model for the modelling of gas-solid fluidized beds is proposed. The model is a revision of the Particle bed Model proposed by Foscolo and Gibilaro (1987). The mono component equations proposed by Jackson (2001) form the basis of the current model. The initial derivation is for a mono component system. The key features of the new formulation herein include a new dynamic expression for the elastic force as well as a new interphase transfer function that is independent of the drag co-efficient. Features such as the buoyancy force in the original formulation have been retained in this model.

6.1 EQUATIONS OF CHANGE

- **Fluid Phase Equations of Change**

$$\frac{\partial}{\partial t}\left(\varepsilon \cdot \rho_f\right) + \vec{\nabla} \bullet \left(\varepsilon \cdot \rho_f \cdot \vec{U}_f\right) = 0 \quad (2)$$

$$\frac{\partial}{\partial t}\left(\varepsilon.\rho_f.u_f\right) + \left[\nabla \bullet \varepsilon.\rho_f.u_f.u_f\right] = -\varepsilon.\nabla p_f + \varepsilon\tau_f - \beta\left(\mathbf{u}_f - \mathbf{u}_s\right) - E.\left[\nabla\varepsilon \bullet n_D\right].n_D + \rho_f.\varepsilon.\mathbf{g} \quad (3)$$

- **Solid Phase Equations of Change**

$$\frac{\partial}{\partial t}\left(\alpha \cdot \rho_p\right) + \vec{\nabla} \bullet \left(\alpha \cdot \rho_p \cdot \vec{U}_p\right) = 0 \quad (4)$$

$$\frac{\partial}{\partial t}\left(\alpha.\rho_s.u_s\right) + \left[\nabla \bullet \alpha.\rho_s.u_s.u_s\right] = -\alpha.\nabla p_f + \alpha.\tau_f + \beta\left(\mathbf{u}_f - \mathbf{u}_s\right) + E.\left[\nabla\varepsilon \bullet n_D\right].n_D + \rho_s.\alpha.\mathbf{g} \quad (5)$$

6.2 CLOSURE RELATIONSHIPS

- **Interphase Transfer Co efficient**

$$\beta = \left[\left(\frac{17.3}{\mathbf{Re}_p}\right)^{\gamma} + 0.336^{\gamma}\right]^{\frac{1}{\gamma}} \frac{\rho_f\left(\left|\mathbf{u}_f - \mathbf{u}_s\right|\right)}{d_p}(1-\varepsilon)\varepsilon^{-1.8} \quad (6)$$

$$\gamma = 2.55 - 2.1\left[\tanh(20\varepsilon - 8)^{0.33}\right]^3$$

- **Elastic force**

The elastic force is the expression represented by the term, $E.\left[\nabla\varepsilon \bullet n_D\right].n_D$. The force arises under non steady state and non-equilibrium conditions. The original form of the force was proportional only to the elastic modulus, E, which was derived based on only steady state considerations, and the gradient of the voidage (in the vertical direction only), $\frac{\partial\varepsilon}{\partial z}$. (Gibilaro, 2001). In the new formulation a new elastic modulus term, E, has been derived (shown in equation 7) and the elastic force term is expressed in the form $E.\left[\nabla\varepsilon \bullet n_D\right].n_D$ where n_D is the unit vector in the direction of the local drag force given by the expression, $n_D = \frac{F_D}{|F_D|}$, and where F_D is the drag force

$$E = -\frac{2}{3}d_p\left[F_{D,V}\left(-3.8\varepsilon^{-1} + \kappa\right) - (1-\varepsilon)\left(\rho_s - \rho_f\right)g\right]$$

$$F_{D,v} = \left[\left(\frac{17.3}{\mathbf{Re}}\right)^{\gamma} + 0.336^{\gamma}\right]^{\frac{1}{\gamma}} \frac{\rho_f\left(U_f - U_s\right)^2}{d_p}(1-\varepsilon)\varepsilon^{-1.8} \quad (7)$$

$$\kappa = \left\{ -\frac{1}{\gamma^2}\ln\left[\left(\frac{17}{\mathbf{Re}}\right)^{\gamma} + 0.336^{\gamma}\right] + \frac{1}{\gamma}\left[\frac{\left(\frac{17}{\mathbf{Re}}\right)^{\gamma}\ln\left(\frac{17}{\mathbf{Re}}\right) + 0.336^{\gamma}\ln 0.336}{\ln\left(\frac{17}{\mathbf{Re}}\right) + \ln 0.336}\right]\right\} \times \left(\sec h^2\left[20\varepsilon - 8\right]^{0.33}\right) \times 6.6\left(\left[20\varepsilon - 8\right] + 10^{-9}\right)^{-0.67} \times -6.3\left[\tanh\left(20\varepsilon - 8\right)^{0.33}\right]^2 \quad (8)$$

7 TOWARDS THE CFD MODELLING OF BINARY MIXTURES

A fluid-bed stability analysis was been performed on range of Geldart Group A gas-fluidized powders. Values for the minimum bubbling voidage predicted by the newly proposed PBM have been compared with those predicted by the original PBM, the correlation by Jean and Fan (1992) and experimental data obtained by Xie and Geldart (1995) for Geldart Group A powders. A good agreement was found between predictions of the newly proposed PBM and experimental data (error within ± 5 \%) in the "high" range of mean particle diameters (greater than about 90 μm). Following on from this, the present mono component model is currently been extended to cater for binary particle mixtures. The following assumptions have been made in deriving the binary mixture model:

- The effective weight of a binary mixture balances the pressure drop due to friction drag, thus

$$\left(\frac{\Delta P}{L}\right)_D = \left(\frac{\Delta P}{L}\right)_W$$

Where the effective weight is given by:

$$\left(\frac{\Delta P}{L}\right)_W = \left[\phi_1\left(\rho_{p_1} - \rho_f\right) + \phi_2\left(\rho_{p_2} - \rho_f\right)\right]g$$

- The Drag force equation shown earlier in eqn.7 applies to the case of binary mixtures with modifications to the particle diameter, d_p, and the volume fraction occupied by the fluid, ε. The coefficient γ is also assumed to have the same numerical value as one obtained for a mono component bed.

- The particle diameter can be defined with reference to the Sauter-Mean diameter of the mixture, given by.

$$d_{sm} = \frac{1}{\sum \frac{x_i}{d_i}}$$

The above modifications result in a new equation for the Elastic force, defined earlier in eqn 8. However, a longer treatise on the proposed binary mixture model will be published later.

CONCLUSIONS

CFD simulations of two industrial Group B materials have been performed using a commercial code, CFX 4.4. For velocities investigated, a good qualitative match was found between the simulations and experiments. Simulated values for bed expansion were found to be in good agreement with experimentally measured values (within 11%) at the velocities investigated. Experimental results as well as an empirical bubble correlation were used to validate predicted simulation results for bubble size. Similar trends were observed, however for both powders the Darton et al.(1977) empirical correlation was found to over predict the bubble diameters when compared to experimental and simulated values.

A new Particle Bed model has also been proposed. Stability analysis performed on the mono component model showed a good agreement with the experimental data of Xie and Geldart (1995). The newly proposed model is currently been extended to cater for binary mixtures.

NOMENCLATURE

d	diameter, m
E	Elastic Modolus
u	velocity, m/s

Greek Letters

β	inter-phase drag, kg/m^3 s
ε	volume fraction
γ	Di Felice drag function,
γ	drag function exponent,
ρ	density, kg/m^3
μ	viscosity, kg/m s

Subscripts and superscripts

1	*particle 1*
2	*particle 2*
f	*fluid phase*
g	gas phase
n	exponent
p	particle
s	solid phase
D	drag

REFERENCES

CAMMARATA , L., LETTIERI, P., MICALE,.G., COLEMAN, D., (2003b), 2D and 3D CFD simulations of bubbling fluidized beds using Eulerian-Eulerian models. IJCRE 1(A48) 1-19

DARTON, R. C., LANAUZE, R.D., DAVIDSON, J.F., HARRISON, D., (1977), Bubble growth due to coalescence in fluidised beds, Trans IChemE, 55, 274-280

DING, J, GIDASPOW, D.,(1990), A bubbling fludization model using kinetic theory of granular flow, AIChE Journal, 36, pp.523-538.

FOSCOLO, P., GIBILARO, L., (1987). Fluid Dynamic Stability of fluidised suspensions: The Particle Bed Model . *Chem. Eng. Sci*, 42, 1489.

FOSCOLO, P.U., GIBILARO, L.G., (1984), A Fully Predictive Criterion for the Transition Between Particulate and Aggregate Fluidization, *Chem. Eng. Sci.,* 39, pp. 1667.

GIBILARO, L.,(2001). Fluidization dynamics. Butterworth-Heinemann.

GIDASPOW, D., (1994), Multiphase Flow and Fluidization; Academic Press London.

JACKSON, R., (2001). The dynamics of Fluidized Particles. Cambridge University Press, New York USA.

JEAN, R., and FAN. F,.(1992). On the model equations of Foscolo and Gibilaro with corrected buoyancy force. *Powder Technology*, 72, 201-205

KUNII, D., LEVENSPIEL, O (1989), Fluidization Engineering, Butterworth-Heinemann, Second Edition

LETTIERI, P., (1999), BRANANI, S., YATES, J., AND NEWTON, D.(2001) A generalization of the Foscolo and Gibilaro particle bed model to predict the fluid bed stability of some fresh FCC catalyst at elevated temperatures. *Chem Eng. Sci*,56, 5401-5412.

LETTIERI, P., CAMMARATA , L., MICALE, G., YATES, J.,(2003a), CFD Simulations of Gas Fluidized beds using alternative Eulerian-Eulerian modelling approaches IJCRE, 1, A5

OWOYEMI. O., LETTIERI P., WESTWOOD., M, (2005), Towards the CFD Modelling of Bimodal Gas Fluidized Beds, In Proc: CFD in Chemical Reaction Engng. IV Conf, Barga, Italy.

VAN WACHEM, B., SCHOUTEN, J.C., VAN DEN BLEEK, C.M., KRISHNA, R., (1998), Eulerian simulations of bubbling behaviour in gas-solid fluidized beds, Computer Chem. Engng., 22 Suppl., S299-S306

XIE, H.Y., GELDART, D., (1995), Fluidization of FCC Powders in the Bubble-Free Regime: Effect of Types of Gases and Temperature, *Powder Technology*, 82, pp. 269.